Seismic Performance of Lightly Reinforced Concrete Exterior Beam-Column Joints

Kimreth Meas[1], *Bing Li*[1,*] *and Iswandi Imran*[2]

[1]*School of Civil and Environment Engineering, Nanyang Technological University, Singapore*

[2]*Faculty of Civil and Environmental Engineering, Institute Technology Bandung, Indonesia*

[*]*Corresponding author. Email address: cbli@ntu.edu.sg; Tel: +65-67905090. Associate Editor. J.G. Dai.*

Abstract

This paper presents the experimental results of four lightly Reinforced Concrete (RC) exterior beam-column joints with and without beam stubs under cyclic loading with constant column axial force applied at the top of the column. The parameter investigated was the type of reinforcement used in the beam, i.e. plain and deformed bars. Test results showed that when the hooks anchored down in the column increased the tensile stress in the diagonal concrete strut in the joint core, this led to diagonal crack of the concrete and a decrease in the joint shear strength. The seismic performance of the exterior RC joints without beam stub was also observed to be much improved when the hook tail of beam reinforcements was bent inside the joint core. The strut-and-tie model based on the recorded strain in the joint transverse reinforcement could be used to determine the force flow in the joint core.

Keywords: reinforced concrete, beam-column joints, seismic performance.

1. Introduction

Under seismic loading, the RC beam-column joint core is subjected to horizontal and vertical forces which are many times larger than the beam or column elements. If the joint core is not carefully designed and detailed, it may become the weak link amongst the structural elements (Li *et al.* 2002, 2009). This can have a significant effect on the overall response of the structure and can even reduce the ductility performance, as reported by Dadi and Agarval (2008). A common structural system used for houses in Indonesia consists of reinforced concrete frames with masonry infill. The concrete frames are usually lightly reinforced. In several recent earthquakes in Indonesia such as the Yogyakarta earthquake (M 6.3) of 27 May 2006, the Padang earthquake (M 7.6) of 30 Sep 2009, etc., many structures of this form experienced failure, as investigated by Imran *et al.* (2006). Most of the failures were due to masonry wall collapse, initiated by anchorage failures of the RC frame elements. This might be because the size of the columns framing the RC beam-column joints was not large enough and thus the dowel action could not be

fully developed. As a result, the joint core could lead to bond stress deterioration. Secondly, the majority of the reinforcing bars used were plain bars. It was common practice in Indonesia to use columns of size 100 mm $\times$ 100 mm or 150 mm $\times$ 150 mm in the construction of low-rise buildings. However, this was an unsound practice as it was not in conformity with the Indonesia Concrete Code, SNI 03-2847-02, (Purwono *et al.* 2007). According to SNI provisions, which have similarities with ACI 318-08, the size of the columns framing the joint core should not be less than twenty times the diameter of the beam rebars (d_b) crossing the joint for interior joints and approximately $15d_b$ + cover thickness for exterior RC joints. Plain bars may need bigger columns in order to carry the bond stress developed in the joint core. Coupled with smaller column sizes, this could lead to bond slips in the joint core at low levels of lateral loads. Different types of hooks bent in the joint core can also affect the performance of the joint. Priestley (1997) indicated that the seismic behaviour of the exterior RC beam-column joint with deformed beam bar with 180-degree hooks in the joint core performed better than that with hooks of the beam bar bent out of the joint core. A research on the use of plain round bars with 180-degree hooks and no transverse reinforcement in the exterior RC joint showed significant brittle failure after diagonal crack of the joint core (Pampanin et al. 2002). After the recent earthquakes in Indonesia, such as the Great Sumatra Andaman Island earthquake of 2004, the Department of Public Work of Indonesia (DPW) published a new set of guidelines for designing earthquake-resistant houses (Dept of Public Work 2005). At present, this set of guidelines has already been adopted for the construction industry in Indonesia. However, the performance of the proposed RC joint detailed from this guideline needs to be better understood. For instance, the guideline still allows the use of plain bars as the main reinforcement in frame elements. Furthermore, no special treatment has been proposed to improve the bond capacity in the joint core. It should be noted that the DPW guidelines never specify the minimum size of structural columns, but they specify how the detailing should be carried out in the joint area. According to the DPW guidelines, all hooks of the beam bars framing the exterior beam-column joints should be bent down in the column. It is interesting to see how the joints perform seismically with this kind of detailing. Furthermore, since the DPW guidelines do not limit the minimum size of structural columns in the exterior joints, the exterior joint area may become prone to shear failure when subjected to seismic loads. One way to prevent this is by providing beam stubs to anchor the beam bars framing the exterior joints. Unfortunately, the volume of experimental research available on exterior RC beam-column joints using all hooks of the beam bar, bent down in the column or extended into the beam stub with this particular detailing, is rather limited so far.

Therefore, an experimental program on two test specimens without beam stub and one specimen with beam stub of exterior RC beam-column joints designed according to the guidelines of the Department of Public Work (DPW 2005) was carried out. A fourth specimen with beam stub and deformed bar in the beam, designed in accordance with the Indonesian code for concrete buildings, SNI 03-2847-02, (Purwono *et al.* 2007) was also tested. Figure 1 shows the typical school building in Padang, Indonesia.

2. Test Programme

Four full-scale specimens of exterior RC beam-column joints representing the moment-resisting frame of a building were tested. For these specimens, the beam length and column height were taken as half of the beam length and the column height in the frame in which the beam and column ends were the points of inflection under the applied lateral load. The beam length was measured as 2.4 m from the column axis to the point of inflection while the column height was measured as 2.9 m from the bottom support to the point of load application. One specimen without beam stub with the hook of the beam bar as plain bar anchored down into the column was designed following the recommendation of the DPW guidelines while another specimen was identical with the previous one, but with an additional beam stub. These specimens were tested in order to evaluate whether the additional beam stub could improve the test performance. Similarly, two additional exterior RC joint specimens of similar geometry but reinforced with deformed bars were also tested. One of these specimens, i.e. the one with beam stub, was designed in accordance with the Indonesian code for concrete buildings, while the other one (without beam stub) was detailed in accordance with the PWD guidelines.

2.1. Description of Test Specimens

Deformed bars were used in the columns for all the four specimens. Two characteristics of the specimens were varied as follows: (a) use of deformed bar or plain bar in the beam; (b) hooks of beam bars bent down into the column or beam stub. The specimens were labelled with letters. The first letter was either P – indicating the use of plain bars in the beam – or D – indicating the use of deformed bars in the beam. The second letter was either B – indicating that the hooks of the beam bars were anchored in the beam stub – or C – indicating that the hooks of the beam bars were anchored down into the column. As such, the specimens were labelled as DB, PB, PC and DC. The beam and column sections of all specimens were 150 mm × 200 mm and 200 mm × 200 mm, respectively. The specimens were basically a full-scale model of a typical exterior beam-column joint of two-story residential buildings located in a zone with moderate level of seismic risk in Indonesia. The detailing of specimen DB is in accordance with SNI 03-2847-02, (Purwono *et al.* 2007) while the detailing of the remaining specimens is in accordance with the DPW guidelines.

2.2. Reinforcement Details

The reinforcement details of DB and PB are shown in Figure 2 while Figure 3 shows the reinforcement details of specimens DC and PC. The beam sections of all specimens were symmetrically reinforced. The columns for all specimens were symmetrically reinforced with two deformed longitudinal reinforcements of 10 mm diameter. A plain bar of 10 mm diameter was used for beam and column transverse reinforcement. Two layers of 10 mm diameter plain bars were also used as transverse reinforcement in the joint core with 77 mm spacing. The total

area of transverse reinforcement required by ACI 318-08 Sect. 21.4.4 was 206 mm^2, the same as that in the column. The total area was calculated using Eqn 1:

$$A_{sh} = 0.3\,(sh_c' f_c' / f_{yh})\,[(A_g / A_{ch}) - 1] \quad (1)$$

But not less than Eqn 2:

$$A_{sh} = 0.09(sh_c^{'}\ f_c^{'} / f_{yh}) \quad (2)$$

For this specific detailing in the joint core of the specimen, the total area of transverse reinforcement was about 157 mm^2. The joint transverse reinforcement ratio was 1.2%. This was about 24% less than that required by ACI 318. Nevertheless, it should be noted that the amount of the transverse reinforcement provided in the test specimens was still larger than that proposed by the DPW guidelines which recommend the maximum spacing of transverse reinforcement in the plastic hinge regions of beam and column to be ($^{h}/_{2}$). It is a common practice to use transverse reinforcement of the same size as that of rebars in Indonesia.

2.3. Material Properties

The deformed bar used in the column and beam as longitudinal reinforcement was characterized by a yield strength f_y equal to 553 MPa. A plain round bar of 10 mm diameter with yield strength f_{yh} equal to 333 MPa was used for transverse reinforcement and longitudinal reinforcement in the beam for specimens using a plain bar. The compressive strength of the concrete cylinders corresponding to the time when the specimens were tested was about 33 MPa for all specimens. The typical yield strength commonly used in Indonesia ranged between 400 to 500 MPa for deformed bars and between 240 to 320 MPa for plain bars. The typical concrete strength used in standard practice in Indonesia was usually around 20 MPa. The Indonesian concrete code limits the concrete strength for earthquake-resistant structures to be no less than 21 MPa. As it was difficult to obtain concrete with this strength in Singapore, concrete strength of 33 MPa was used in these specimens. This compressive strength $f_c^{'}$ was obtained by averaging the compressive strengths of the cylindrical samples. Table 1 shows the reinforcing steel properties.

2.4. Nominal Capacities

Material properties obtained from the sample tests were used to design the flexural strength of the beam and column. All the specimens were designed to satisfy the "strong column-weak beam" philosophy in ACI-ASCE 352 (2002), which limits the minimum column-to-beam moment ratio to 1.2. The column-to-beam moment ratios and other design parameters are shown in Table 2. When the external load is applied to the structural frame, the beam and column introduce internal stresses at the joint faces, which might lead to the diagonal crack of concrete if the shear strength of the joint core is not sufficient. Due to the internal stresses from the beam and column at the faces of the joint core, the horizontal and vertical joint shear stresses v_{jh} and v_{jv} are assumed to

act at the centre of the joint core. The joint shear stress is assumed to be resisted by the diagonal compression struts of the concrete and the truss mechanism by transverse reinforcement. The truss mechanism sustains the forces transferred by the beam and column main bars, provided that the bond condition is good enough (Park and Paulay 1975). When the joint core reaches its maximum stress, these joint shear stresses will become the principal tensile and compressive stresses, f_{dt} and f_{dc}. The critical failure in the joint core is dominated by the principal tensile stress expressed in terms of the horizontal joint shear stress as shown in Eqn 3:

$$f_{dt} = \frac{\sigma_a}{2} - \sqrt{\left(\frac{\sigma_a}{2}\right)^2 + \left(v_{jh}\right)^2} \tag{3}$$

Where σ_a = column axial stress ($\frac{N}{A_g}$); V_{jh} = joint horizontal shear stress ($\frac{V_{jh}}{A_j}$)

where A_j is the effective joint area which is taken as (b_b + 2x) h_c without considering the length of the beam stub in the case of the joint with a beam stub. And $V_{jh} = T_b - V_c = 1.25A_s f_y - V_c$.

A coefficient of 1.25 is taken into account in this formula as it is widely used in New Zealand (Park and Paulay 1984) when beam strength reaches its overestimated magnitude with the occurrence of plastic hinge in the beam. Previous experimental studies had been done on the exterior RC beam-column joints by the use of plain bar and without joint transverse reinforcement (Pampanin *et al.* 2002). The result showed that the joint core would reach its maximum stress at a principal tensile stress of $f_{dt} = 0.2\sqrt{f_c'}$ (MPa) when beam reinforcement was in the form of plain round bars. The maximum stress in the joint core reached a principal tensile stress of $f_{dt} = 0.29\sqrt{f_c'}$ (MPa) in the joint core without transverse reinforcement when the hook of deformed beam bar was bent out of the joint core as tested by Priestley (1997). Even though the principal tensile stress was used to predict the joint shear strength, the current code and other researchers expressed the horizontal joint shear stress in terms of v_{jh}. Park (2001) investigated the seismic performance of exterior RC beam-column joints without column axial force. In these specimens, the beam bars were deformed bars and low transverse reinforcement was used in the joint region. The result showed that the maximum horizontal joint shear stress v_{jh} was $0.31\sqrt{f_c'}$ (MPa) when the hooks of the beam bars were bent inside the joint core. The maximum horizontal joint shear stress v_{jh} was $0.25\sqrt{f_c'}$ (MPa) when the hooks of the beam bars were bent out of the joint core (Park 2001). It should be noted that Eqn 3 is valid only when the column is under compressive load, and not tensile load.

2.5. Test Setup

Figure 4 shows the test setup of the specimens, each of which was subjected to a constant axial load of 0.1 $f_c' A_g$ and quasi-static load reversals that simulated earthquake loading. The bottom of the column was pinned to the strong floor of the laboratory and the end of the beam was also

connected to this strong floor by steel links, which provided restraint against vertical translation but allowed for horizontal translation of the beam. A reversible horizontal load was applied to the column using a hydraulic actuator, which had a capacity of 50 tons. The specimens were under quasi-static cyclic loading with displacement control. The lateral load sequences consisted of two cycles to each story drift ratio (DR), from a DR of 0.25% to 4.5%. An increment of 0.25% was used from a DR of 0.25% to a DR of 3% and then 0.5% until a DR of 4.5%. The drift ratio was considered to be the ratio of horizontal story displacements at the top of the column to the total column height. The displacement history is shown in Figure 5.

In order to improve the accuracy of the test results, instruments such as the actuator, strain gauges and Linear Displacement Transducers (LVDT) were installed on all specimens during the test setup. The behavior of the reinforcing bars was monitored by the strain gauges installed on the bars prior to casting concrete. Figure 6 shows the arrangement of the strain gauges on the reinforcement while Figure 7 shows the arrangement of the displacement transducers that measured the shear deformations of joints and the flexural deformations of beams and columns. The transducers were mounted on steel brackets.

3. Experimental Results and Observations

The following sections describe the experimental observations and analytical results from the test conducted on all four specimens. The observed yield and ultimate strength with the corresponding drift ratios of all specimens are presented in Table 3. P_{th} is the theoretical horizontal load at the top of the column associated with the theoretical flexural strength of the beam, as shown in Figure 8. The theoretical flexural strength is calculated using the conventional compressive stress block for the concrete with an extreme fibre concrete compressive strain of 0.0035 and the steel yield from the test. The definition of theoretical initial stiffness K_{th}, widely used in New Zealand practice, is also shown in the figure.

3.1. Specimen PB: Plain Beam Bar and Beam Stub

As shown in Figure 9, PB attained its approximated theoretical horizontal strength of 4.5 kN at a DR of about 1.0% in both the loading directions and theoretical initial stiffness of 0.21 kN/mm. The specimen attained its yield strength of 3.87 kN at a DR of almost 1.0 % equivalent to horizontal displacement of 23 mm in the positive loading direction at the start of the yielding on the beam reinforcement. Therefore, at the time of yielding of the beam reinforcement, the stiffness from the experimental testing was 0.16 kN/mm, which was 23.8% lower than the theoretical initial stiffness. At a DR of 4.0%, it attained the maximum horizontal load of 6.18 kN in the positive direction of loading, while in the negative loading direction it attained the maximum horizontal load of -7.46 kN at a DR of -4.5%. The approximate theoretical strength was 27.2% lower than the measured maximum shear strength in the positive direction of loading. The specimen showed ductile behavior with little strength decrease by reaching 95.8% of its

maximum shear strength in the last positive DR of 4.5%. The observed crack pattern is shown in Figure 10. Specimen PB exhibited flexural cracks on the beams at an early stage at a DR of 0.25%. No crack was observed on the column and joint core even at higher DR. However, severe flexural cracks appeared on the beams. Cracks on the beam stub of this specimen started at a DR of 2.25%. This crack development continued extensively until the last story drift ratio was 4.5%. This showed that the bond along the joint area was not effectively developed to resist the tensile force from the beam reinforcement due to the yielding of beam reinforcement in the beam stub. The strain profile of beam reinforcement is shown in Figure 11. This was also due to the fact that the cross-section of the plain bar in the beam experienced contraction from the effect of Poisson's ratio during tension. As a result, the bond mechanism of the plain bar, which consisted of only adhesive and frictional mechanisms, would be reduced significantly. Figure 12 shows the displacement decomposition ratio of specimen PB until a DR of 2.0%. In this figure all deformations are transferred to drift contributions, in percentage to total drift of the column. At a DR of 2.0%, the beam contributed the largest deformation of about 83.1% amongst all the components. The definition of the displacement decomposition of each component to the column deformation is shown in Figure 13. The deformation of each component was calculated using the data from the transducers installed on the specimens as shown in Figure 7. Different displacement components can be estimated according to the measured member curvatures and the joint shear distortion as reported in the research report 2002-1 by Aizhen Liu (2002).

3.2. Specimen PC: Plain Beam Bar and No Beam Stub

PC also attained its approximate theoretical horizontal strength of 4.5 kN at a DR of around 1.0% in both loading directions and approximate theoretical initial stiffness of 0.21 kN/mm as shown in Figure 9. The observed stiffness from the testing at the yielding of the beam reinforcement was 0.15 kN/mm, which was 27.3 % lower than the approximate theoretical initial stiffness. The maximum horizontal load attained at a DR of 2.25% in the positive loading direction was 4.93 kN. In the negative loading direction, the maximum horizontal load reached was about −7.1 kN at the last DR of −4.5%. In the following positive loading cycles, the specimen showed ductile behavior with more strength decrease at the last DR of 4.5% by reaching only 73% of its ultimate shear strength. Flexural cracks were also observed from the early stage at a DR of 0.25% on the beam. No crack was observed at the joint core while the beams experienced severe damage. The observed crack pattern of this specimen is shown in Figure 10. After reaching the maximum shear strength at a DR of 2.25%, the specimen showed severe cracking of the conic column concrete cover on the face of the joint core away from the beam. It was because of the slip of the beam bars within the joints that caused the beam bars to bear on the concrete cover of the column. The strain profile of beam reinforcement is shown in Figure 11. During testing, the beam showed the maximum deformation, which can be clearly seen from the displacement decomposition ratio calculated up to a DR of 2.0% from Figure 12. At a DR of 2.0%, the beam contributed the most deformation of around 85.3%. No yielding of the column reinforcements and transverse reinforcements in the joint core were observed. The definition of the displacement

decomposition of each component to the column deformation is shown in Figure 13. The deformation of each component was calculated using the data from the transducers installed on the specimens as shown in Figure 7.

3.3. Specimen DB: Deformed Bar and Beam Stub

Figures 9 and 10 show the hysteresis loops and crack pattern of specimen DB respectively. The experimental result showed that DB attained its approximated theoretical ideal horizontal strength of 6.5 kN at a DR of 1.5% in the positive loading direction. At a DR of 2.5%, it attained the maximum horizontal load of 8.07 kN in the positive direction of loading, while in the negative direction of loading it attained the maximum horizontal load of 9.4 kN at a DR of −4.5%. This indicated that the approximate theoretical strength was 18.6% lower than the observed maximum shear strength in the positive direction of loading. The theoretical stiffness was 0.20 kN/mm. The observed stiffness from experimental testing at the start of yielding of the beam reinforcement was 0.13 kN/mm, 35% lower than the theoretical stiffness. The strain profile of beam reinforcement is shown in Figure 11. At the final DR of 4.5%, the specimen showed ductile behavior, carrying strength corresponding to approximately 93.5% of its maximum shear capacity. The hysteresis loops exhibited stable and ductile behavior throughout the test. The first flexural crack occurred on the beam at a DR of 0.25%. The fine crack was observed on the column at a DR of 2.25% with very little crack development at the last DR. As shown in Figure 12, the beam exhibited the most deformation of about 73.5% at a DR of 2.0%. The definition of the displacement decomposition of each component to the column deformation is shown in Figure 13. The deformation of each component was calculated using the data from the transducers installed on the specimens as shown in Figure 7.

3.4. Specimen DC: Deformed Bar and No Beam Stub

As shown in Figure 9, DC attained its approximate theoretical strength of 6.5 kN at a DR of 1.5% in both loading directions and approximate theoretical initial stiffness of 0.18 kN/mm. The maximum horizontal load from the testing was 7.25 kN at a DR of 2.75% in the positive loading direction, while in the negative loading direction, the maximum horizontal load gained was about −8.96 kN at a maximum DR of −4.5% without strength decrease. This showed that the approximate theoretical strength was 10.34 % lower than the observed maximum shear strength in the positive direction of loading. The stiffness from the experimental testing at the start of yielding of the beam reinforcement was 0.14 kN/mm, which was 22% lower than the theoretical stiffness. In the last positive loading cycles, the specimen showed ductile behavior with little strength reduction, attaining 96% of its maximum capacity. The hysteresis loop showed some pinching behavior due to the diagonal crack observed in the joint. After reaching the shear strength at a DR of 2.25%, the specimen attained principal tensile stress of $0.24\sqrt{f_c'}$ (MPa). This was due to the fact that in the positive loading direction, the bottom beam bars sustained a tensile force, causing the hooks of the beam bars anchored down into the column to move away from the joint core. Such a move increased the diagonal tensile and compression force and resulted in

a diagonal crack. After lateral load reversals, the specimen showed only little strength decrease of about 6.5% at the maximum drift ratio without much crack propagation. This was due to the truss mechanism resisting the joint shear instead of the concrete strut mechanism after the diagonal concrete crack. The observed crack pattern is shown in Figure 10. From the displacement decomposition ratio as shown in Figure 12, at a DR of 2.0 %, the beam contributed the largest deformation of about 72.0%. The definition of the displacement decomposition of each component to the column deformation is shown in Figure 13. Even though there was diagonal crack of concrete, all the transverse reinforcements were yet to reach their yielding strain of 0.00158. The strain profile of the beam reinforcement is shown in Figure 11.

4. Discussion on Experimental Observations

4.1. Loading Capacities and Hysteresis Responses

From the hysteresis loop as shown in Figure 9, PB and PC reached their maximum capacities at the ductility of 4.0 and 2.0 respectively in the positive direction of loading. Specimen PB exhibited more ductile behavior and a higher maximum shear capacity than that of PC. Greater strength reduction was observed particularly for PC, with the hooks of the beam bar bent downwards in the column. Its measured maximum shear strength was about 20.22% lower than that of PB with the hooks of the beam bar bent inside a beam stub. The stiffness degradation of PC was more significant than that of specimen PB, as shown in Figure 14. The lower performance of PC was probably due to the slip of the beam bar in the joint core, resulting in cracking at the column face due to the dowel action of the beam bar to the column concrete cover.

For DB with the hooks of the beam bars bent inside the beam stub, its maximum shear strength was 10% higher than that of DC with the hooks of the beam bars bent downwards in the column. From the hysteresis loop as shown in Figure 9, DB had a higher maximum capacity than that of DC at almost the same ductility of 1.5. The better seismic performance of the exterior beam-column joint with beam stubs can be attributed to the concrete stub providing the bearing to the secondary struts in the joint core. This will reduce the concentration of force in the major strut. The initial stiffness of 0.13 kN/mm of DB obtained from the experiment was 15.38% higher than that of DC which was 0.11 kN/mm. The stiffness degradation of specimen DC was higher, as shown in Figure 15.

As illustrated in Figure 16, exterior RC joints using deformed reinforcements in the beam had higher strength and stiffness than that using a plain bar. Severe slip of the beam bar anchorage in the joint region and beam stub was observed for specimens with plain round bars as longitudinal reinforcement in the beam.

4.2. Column Behavior

The columns for all the specimens were designed to avoid development of plastic hinges, following the recommendation of ACI-ASCE 352-02 (2002) with the lower limit of the column-to-beam flexural ratio of 1.2. In this research study, the columns were designed with a column-to-beam flexural ratio of 2.67 for exterior RC joints with longitudinal deformed bar in the beams of DB and DC, while the ratio of 4.36 was for exterior RC joints with a plain round bar in the beams of specimens PB and PC. The longitudinal reinforcement ratio expressed in terms of the column cross-sectional area is 0.79%, which was lower than the minimum ratio of 1% required by ACI 318-08 (2008). Even though there were fine cracks occurring in the column near the joint of specimens using a deformed bar, the strain of the main reinforcement of the columns of all specimens was much lower than its yield strain.

4.3. Beam Behavior

The beams of all specimens were designed to allow plastic hinges to form in the beam in which the longitudinal reinforcement ratio was $\rho = \rho'$ =0.52% on top and at the bottom. The beam stirrup ratio was 2.9% when the stirrup spacing was 50 mm. The beam stirrup ratio is the ratio of the cross-sectional areas of two legs of stirrup to the area formed by the spacing of the stirrup and beam width excluding the concrete cover. The spacing for all the stirrups in the beam was in accordance with the recommendation by the DPW guidelines, i.e., the maximum spacing of transverse reinforcement in plastic hinge regions of beams is $h/2$. Strain hardening was observed in the beam reinforcement. During testing, flexural failure was the dominant mode of failure in the beams of all specimens. The horizontal shear strength of the specimen in the positive loading direction was lower than that in the negative loading direction. When the load was applied in the positive direction, the bottom beam bars were in tension. However, the hook tail anchored down in the column was in the compression zone of the column concrete. This would delay the tension force in the hook tail when complete tension was required to resist the tension force from the bottom beam bars. To achieve this, the hooks of the bottom beam bars should be bent upwards in the joint core. Shear cracking in the beam did not occur due to the low shear stress in the beam and before cracking, the reinforcement experiences very little stress.

4.4. Joint Behavior

The nominal joint shear for seismic design can be calculated by using Eqn 4 from the ACI 318b code by removing the safety coefficient of 0.85.

$$V_n = \gamma \sqrt{(f_c')} A_j \tag{4}$$

where γ = 1 for exterior joint for this specimen; A_j is the effective area of beam-column joint (mm^2).

The amount of transverse reinforcement in the joint was 24% less than the minimum requirement provided by ACI 318. The maximum shear strengths of the joints for all specimens were dominated by the beam flexural strength, which was determined by the yielding of beam bars. Especially for DC, at a DR of 2.25% in the positive loading direction, the first diagonal tensioned crack appeared. Cracking was due to the hooks of the beam bars, bent downwards into the column. This caused inherent tension to the diagonal concrete strut. In spite of the diagonal crack in the joint core, the specimen attained its maximum capacity at a DR of 2.5%. The specimen reached its joint shear stress at a principal tensile stress of $0.24\sqrt{f_c'}$(MPa) with a corresponding joint shear stress of v_{jh}=$0.44\sqrt{f_c'}$ N/mm^2 calculated taking into account of 1.25 times after the yielding of the beam reinforcement. At the last DR, the yielding of the transverse reinforcement was not developed in the joint. In comparison with the previous research by Priestley (1997), whereby the beam bar was the deformed bar, the joint without joint reinforcements reached a principal tensile stress of f_{dt}=$0.29\sqrt{f_c'}$ (MPa) when the hooks of the beam bars were bent out of the joint core. This principal tensile stress obtained from the experiment by Priestley (1997) was 17.3 % higher than the experimental result of this study. Even though the transverse reinforcement ratio in the joint was 24% lower than that required by the ACI code, the joint shear strength still increased with ductile behavior after concrete crack of the joint core. However, some researchers' interpretation of the total joint transverse reinforcement ratio was different from the recommendation in the ACI code. Wong and Kuang (2008) confirmed that the upper limit of the horizontal joint core link ratio for enhancing the shear capacity of the exterior beam column joint was 0.35%. The total horizontal joint core link ratio in this tested specimen was 0.78%, which was two times larger than the recommended value by Wong and Kuang (2008). This upper limit value agreed well with that suggested by Kitayama *et al.* (1991), which was 0.4% of the hoop ratio for the case of interior beam column joints. In the negative direction of loading, 90 ° bent hooks were observed to demonstrate more effective bearing, enhancing the joint shear strength. No crack was also observed in the joint core. The joint cores of both specimens using the deformed bar showed elastic behavior throughout the test in both directions.

4.5. Bond Condition of Beam Bar in the Joint Core

Even though the column dimension met the ACI 318-8 requirements, i.e. the column depth should not be less than 20 times the diameter of the beam rebar, during the experiment, bond deterioration of the tensile beam rebar in the joint core was observed through the horizontal crack on the column along the beam bar in the joint core of DC, as shown in Figure 10. To identify the differences of the bond deterioration condition amongst the specimens, beam bar diameter-to-column depth ratio was considered as the main factor. By using the development length instead of column depth, the relation between the development length and beam bar diameter could be determined from the ACI Code 318M-08 (2008) for deformed bars, as shown in Eqn 5:

$$L_{dh} = \frac{f_y d_b}{5.4\sqrt{f_c'}} \quad (5)$$

From this equation, the required development length for specimens using the deformed bar was calculated to be 178 mm and the hook length was $12d_b$ = 120 mm. It can be seen that the exterior RC joint with beam stub provided sufficient development length for longitudinal beam bars. For the exterior RC joint without beam stubs, the required development length was generally sufficient for both top and bottom beam deformed bars in the joint core. However, for the case of specimens using the plain round bar, both specimens showed severe bond deterioration in the joint core. This experimental result showed that for specimen PB, the slip of the beam bar in the joint caused the severe crack in the beam stub while for specimen PC, the wedge formed crack of the column cover at the joint level occurred. For exterior RC joints using plain bars as the main reinforcement in the beam, the ratio of the beam bar diameter to column depth which was the same as that used for the deformed bar was not sufficient.

4.6. Force Transfer Mechanism in the Joint Core

The result showed that the performance of the exterior RC joint with beam stub was better than the one without beam stub, which might be due to the arrangement of reinforcements in the joint core and beam stub.

Figure 17 shows possible strut-and-tie models for the tested specimens based on the recorded forces in the transverse reinforcement of the column within the joint core at maximum response. Based on the strain reading, the strain on the top and bottom transverse reinforcements in the joint core of PB were 6.2E-5 and 2.5E-5 respectively, from which the forces in the top and bottom transverse reinforcements were calculated to be 1.0 kN and 0.4 kN respectively, as shown in Figure 17. For PC, the strains on transverse reinforcements in the joint core were 5.2E-4, 7.1E-4 and 1.2E-4 respectively, from which the forces in the transverse reinforcements were calculated to be 8.3 kN, 11.5 kN and 2.0 kN respectively, as shown in Figure 17. The strains on the top and bottom transverse reinforcements in the joint core of DB were 7.5E-5 and 2.1E-4 respectively, from which the forces in the top and bottom transverse reinforcements were calculated to be 1.2 kN and 3.3 kN respectively, as indicated in Figure 17. For DC, the strains on transverse reinforcements in the joint core were 6.8E-4, 7.5E-4 and 9.3E-4 respectively, from which the forces in the transverse reinforcements were calculated to be 11.0 kN, 12.0 kN and 15.0 kN respectively, as shown in Figure 17. The column and beam forces at each layer of reinforcement acting on the joint core have been calculated from moment-curvature analysis, using the column and beam moments corresponding to the maximum applied story shear force. As shown in Figure 18, column and beam flexural compression resultants combined to form the diagonal joint compression strut. Forces in transverse reinforcements in the joint core and forces in the column and beam longitudinal bars were equilibrated at the core boundary by diagonal struts at an angle with the centroid of the beam and column compression resultants. As shown in

Figure 18, the depth of the major diagonal strut, W_s was calculated directly from the geometrical drawing at the mid-length of the diagonal strut.

For the diagonal compression strut located in the regions where excessive crack was expected, Schlaich et al. (1991, 1987) recommended the allowable concrete stress of $0.34f_c^{'}$ in the case of the interior joint. Based on the above model, the compressive stress within the major diagonal strut of DC was $0.44\,f_c^{'}$, which exceeded the allowable concrete stress of $0.34\,f_c^{'}$. The compressive stress was higher than the allowable stress which might result in diagonal crack in the joint core in the case of the exterior RC joint. This correlated well with the crack pattern of the tested specimen DC. The compressive stress in the major diagonal struts of DB, PB and PC were only $0.28f_c^{'}$, $0.24f_c^{'}$ and $0.30f_c^{'}$ respectively, which were below the allowable concrete stress. It was found from the strut-and-tie model that the force in the major diagonal strut for the exterior RC beam-column joint with beam stub was, on the average, around 34% less than that in the major diagonal strut in the beam-column joint without beam stub. This was due to the increase of the force in the secondary diagonal compression struts, formed by the column and beam flexural compression resultants. These resultant forces were equilibrated by the forces from the beam stub confined by the reinforcement, as clearly shown in Figure 17. Therefore, from the equilibrium condition, this force in the secondary struts reduced the force acting in the major strut. This would allow the major diagonal compression strut to carry more resultant force from the beam and column.

5. Conclusion

Four exterior RC beam-column joints were tested under lateral load reversals to simulate the seismic loading. Two of the joints were with beam stubs and two were without beam stubs. In either type, there was one joint with a deformed bar and the other with a plain round bar in the beam. Based on the experimental results, the following conclusions can be drawn:

(1) For specimens with the hooks of the beam bars anchored down in the column, the bearing of the hooks against the concrete strut in the joint core does depend on the direction of loading. When loading was applied in the positive direction, the hooks of the bottom beam bars were under tension. This force increased the tensile stress of the diagonal strut. It was found that for this specimen using a deformed bar in the beam, the principal tensile stress in the joint core was $0.24\sqrt{f_c^{'}}$ MPa corresponding to the ultimate horizontal joint shear stress of $0.44\sqrt{f_c^{'}}$ MPa. Moreover, in the case when the load was applied in the negative direction, the joint shear strength was enhanced, leading to flexural failure in the beam due to the fact that the joint concrete was confined by the hook of the beam bars and the beam bar in the joint region. Even though the transverse reinforcement in the joint was 0.24% less than that required by the ACI Code, the specimen showed ductile behavior with beam flexural failure.

(2) Through this experimental testing, it was observed that the joint detailing with the hook of the beam bar bent inside the column provided in the DPW guidelines may be improved for better performance. The hook of the beam bar should be bent inside the joint to achieve better performance. This was also confirmed by Priestley (1997).

(3) For both specimens using a plain bar in the beam, severe bond deterioration of the beam bar anchorage in the joint core was observed. The slip of the hooks of the beam reinforcements within the joint core caused cracks in the column concrete cover. Specimens with the plain bars bent into the beam stub attained higher strength and ductility compared to specimens without a beam stub. The horizontal transverse reinforcement in the joint core should be extended up to the hooks of the beam bars in the beam stub in order to prevent concrete crack in the beam stub and to improve the bond condition.

(4) For the specimens with deformed beam bars bent in the beam stub, they exhibited stable spindle hysteresis loop with ductile behavior. Compared with the specimen without beam stubs, the specimen with the beam stub performed better and had higher strength of around 4.7%.

(5) It was shown from the strut-and-tie model that concrete in the beam stub confined by its reinforcement provided a reaction force to the joint core, resulting in increased force distribution in the secondary diagonal concrete strut, and allowing the major diagonal strut to be able to resist more force. Unlike the specimen without beam stub, more force was concentrated only on the major diagonal concrete strut, leading to failure at a lower force than that for the specimen with beam stub.

(6) Due to limited data on this type of anchorage detailing in the joint core, more experimental testing should be carried out to obtain accuracy of the results.

Notation

A_{ch}	the cross-sectional dimension of column core should be measured to the outside edges of the transverse reinforcement composing area of A_{sh}
A_g	gross sectional area of column
A_{sh}	minimum total cross-sectional area of transversal reinforcement
A_j	effective joint area
A_s	reinforcement area
b_b	beam width
d_b	beam bar diameter
$h_c^{'}$	cross-sectional dimension of column core, measured center to center of the confining reinforcement
$f_c^{'}$	concrete compressive strength
f_{dt}	principal tensile stress
f_{dc}	principal compression stress
f_y	yielding strength of main bars
f_{yh}	yielding strength of shear reinforcement
f_u	ultimate strength of reinforcement
f_{uh}	ultimate strength of shear reinforcement
h_c	column depth
h_b	beam depth
L_{dh}	development length of beam bar in the joint
N	column axial force
P_{th}	approximate theoretical horizontal strength
P_u	horizontal strength from experiment
$\Delta_{y,th}$	theoretical initial yield displacement
Δ_{ye}	yield displacement from experiment
Δ_c	deformation due to column
Δ_b	deformation due to beam
Δ_p	deformation due to joint core
K_{th}	theoretical initial stiffness
s	spacing of the transversal reinforcement
T_b	tension force of the beam reinforcement
V_c	column shear force
V_{jh}	horizontal shear force acting in the joint
V_n	nominal joint shear force
v_{jn}	nominal joint shear stress
x	the smallest distance from column edge to beam edge
γ	joint type factor
γ_p	joint distortion
σ_a	column axial stress

References

ACI Committee 318 (2008). *Building Code Requirements for Structural Concrete (ACI 318-08) and Commentary*, ACI 318R-08, Farmington Hills, MI, USA.

ACI-ASCE Committee 352 (2002). *Recommendations for Design of Beam-Column Joints in Monolithic Reinforced Concrete Structures (ACI 352R-02),* Farmington Hills, Michigan, USA.

Liu, A. (2002). *Seismic Assessment and Retrofit of Pre-1970s Reinforced Concrete Frame Structures*, Research Report 2002-1, Department of Civil Engineering, University of Canterbury, Christchurch, New Zealand.

Surya Kumar Dadi, V.V.S. and Agarval, P. (2008). "Cyclic behaviour of exterior beam column joint specimens under quasi-static testing", *Proceedings of the 14th World Conference on Earthquake Engineering*, Beijing, China, pp. 1–8.

Dept. of Public Work (2005). *Practical Guideline for Housing Construction in Earthquake Prone Area*, Department of Public Work, Jakarta, Indonesia.

Imran, I., Suarjana, M., Hoedajanto, D., Soemardi, B. and Abduh, M. (2006). "Lessons from Yogyakarta Earthquake: performance study of buildings (in Indonesian)", *HAKI Journal*, Vol. 7, No. 1, pp. 1–13.

Kitayama, K., Otani S. and Aoyama H. (1991). *Development of Design Criteria for RC Interior Beam-Column Joints. Design of Beam-Column Joints for Seismic Resistance* (SP-123), American Concrete Institute, Detroit, Michigan, USA.

Li, B., Wu, Y.M. and Pan, T.C. (2002). "Seismic behaviour of non-seismically detailed interior beam-wide column joints - Part I: Experimental results", *ACI Structural Journal*, Vol. 99, No. 6, pp. 791–802.

Li, B., Tran, C.T.N. and Pan, T.C. (2009). "Experimental and numerical investigations on the seismic performance of lightly reinforced concrete joints", *Journal of Structural Engineering*, ASCE, Vol. 135, No. 9, pp. 1007–1018.

Pampanin, S., Calvi, G.M. and Moratti, M. (2002). "Seismic behaviour of RC beam-column joints designed for gravity loads", *The 12th European Conference on Earthquake Engineering*, London, UK.

Park, R. (2001). "A summary of results of simulated seismic load tests on reinforced concrete beam-column joints, beam and columns with substandard reinforcing details", *Journal of Earthquake Engineering*, Vol. 6, No. 2, pp. 147–174.

Park, R. and Paulay, T. (1975). Reinforced Concrete Structures, John Wiley & Sons, New York, USA.

Paulay, T. and Park, R. (1984). *Joints in Reinforced Concrete Frames Designed for Earthquake Resistance*, Research Report 84-9, Department of Civil Engineering, University of Canterbury, Christchurch, New Zealand.

Priestley, M.J.N. (1997). "Displacement based seismic assessment of reinforced concrete buildings", *Journal of Earthquake Engineering*, Vol. 1, No. 1, pp. 157–192.

Purwono, R., Tavio, Imran, I., Raka, I.G.P. (2007). *Indonesian Concrete Code for Buildings (SNI 03-2847-2002) with Commentary*, ITSPress, Surabaya, Indonesia.

Schlaich, J. and Schafer, K. (1991). "Designs and detailing of structural concrete using strut-and-tie models", *The Structural Engineer*, Vol. 69, No. 6, pp. 113–125.

Schlaich, J., Schäfer, K. and Jennewein, M. (1987). "Toward a consistent design of structural concrete", *PCI Journal*, Vol. 32, No. 3, pp. 74–150.

Wong, F.H. and Kuang, S.J. (2008). "Effects of beam-column depth ratio on joint seismic behaviour", *Structures and Buildings*, Vol. 161, No. 2, pp. 91–101.

List of Tables

List of Figures

Speci.	Part of Speci.	Longitudinal reinforcement					Transverse reinforcement		
		Deformed bar, mm	Round bar, mm	f_y, MPa	ε_y, (x10^{-6})	f_u, Mpa	Round bar, mm	f_{yh}, Mpa	f_{uh} Mpa
PB and PC	Beam	–	10	333	1586	423	10	333	423
	Column	10	–	553	2633	621			
DB and DC	Beam	10	–	553	2633	621			
	Column	10	–						

Table 1

Specimen	Column flexural strength at applied load of 130 kN, kN-m	Beam flexural strength, kN-m	$\frac{\sum M_c}{\sum M_b}$	P_{th}, (kN)	K_{th}, (kN/mm)
PC and PB ((Plain bar)	24	11	4.36	4.5	0.20
DB and DC (Deformed bar)	24	18	2.67	6.5	0.21

Table 2

Specimen	At first yield		At max. capacity	
	Q_y, kN	DR_y, %	Q_{max}, kN	DR_{max}, %
PB	3.87	1.00	6.18	4.00
			–7.46	–4.50
PC	3.89	1.00	4.93	2.25
			–7.10	–4.50
DB	6.57	1.50	8.07	2.50
			–9.40	–4.50
DC	6.23	1.50	7.25	2.75
			–8.96	–4.50

Table 3

Fig. 1

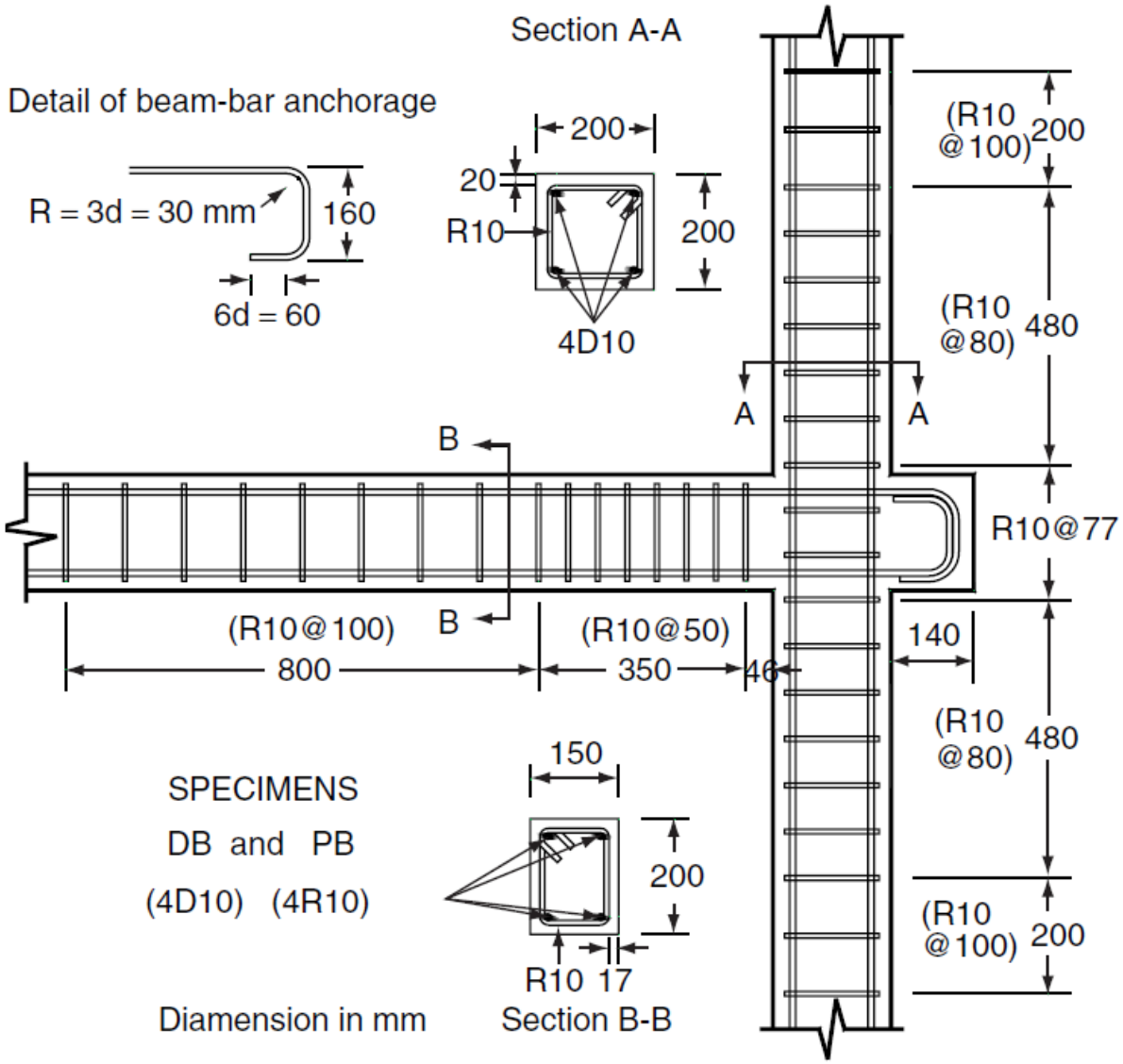
Section A-A
Detail of beam-bar anchorage
R = 3d = 30 mm
160
6d = 60
200
20
R10
200
4D10
(R10 @100)
200
(R10 @80)
480
A
A
B
B
R10@77
(R10@100)
800
(R10@50)
350
46
140
(R10 @80)
480
(R10 @100)
200
150
200
R10
17
SPECIMENS
DB and PB
(4D10) (4R10)
Diamension in mm
Section B-B

Fig. 2

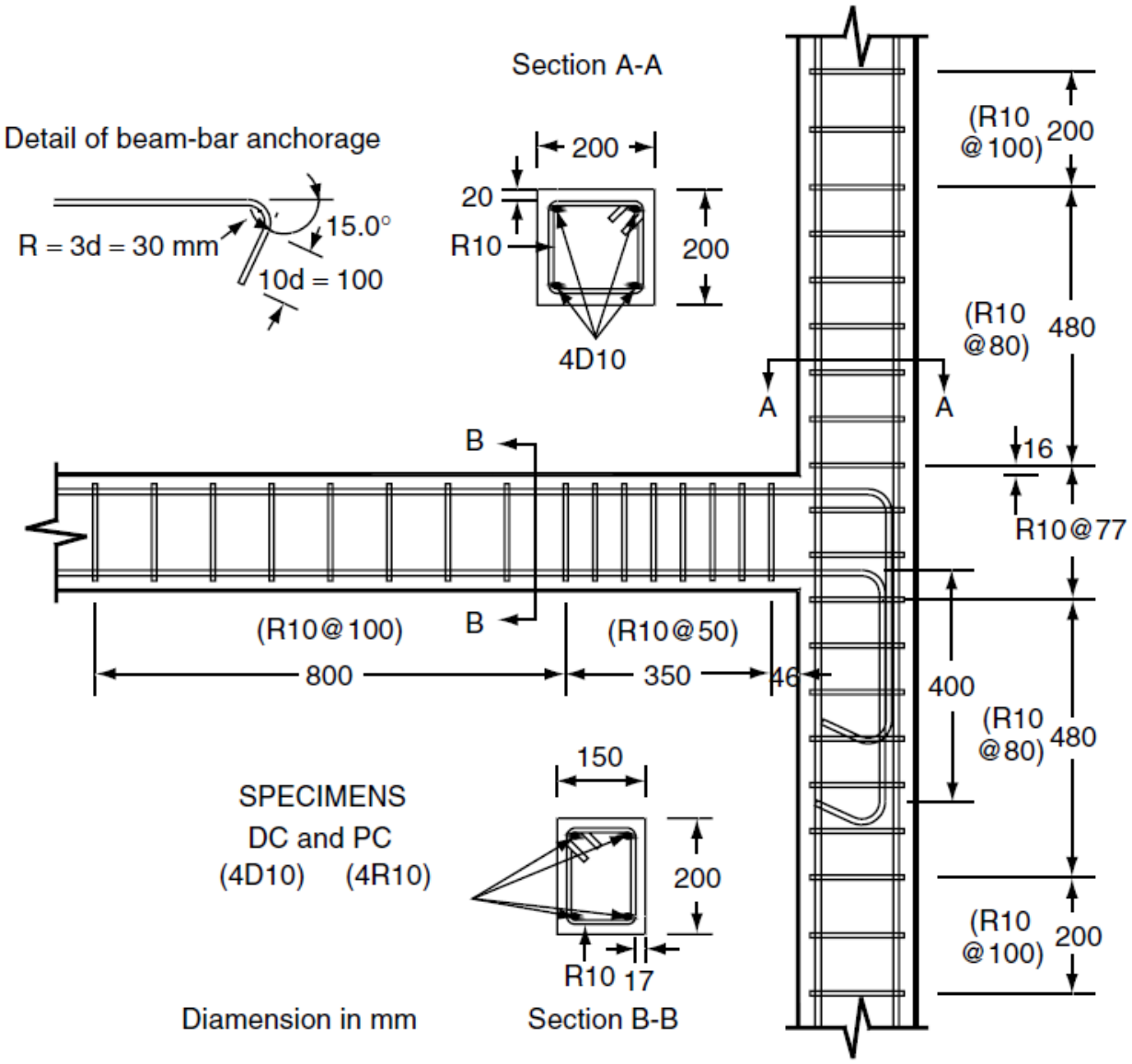
Detail of beam-bar anchorage
R = 3d = 30 mm
15.0°
10d = 100
Section A-A
200
20
R10
200
4D10
(R10 @100)
200
(R10 @80)
480
A
A
B
B
16
R10@77
(R10@100)
(R10@50)
800
350
46
400
(R10 @80)
480
150
SPECIMENS
DC and PC
(4D10) (4R10)
200
R10
17
(R10 @100)
200
Diamension in mm
Section B-B

Fig. 3

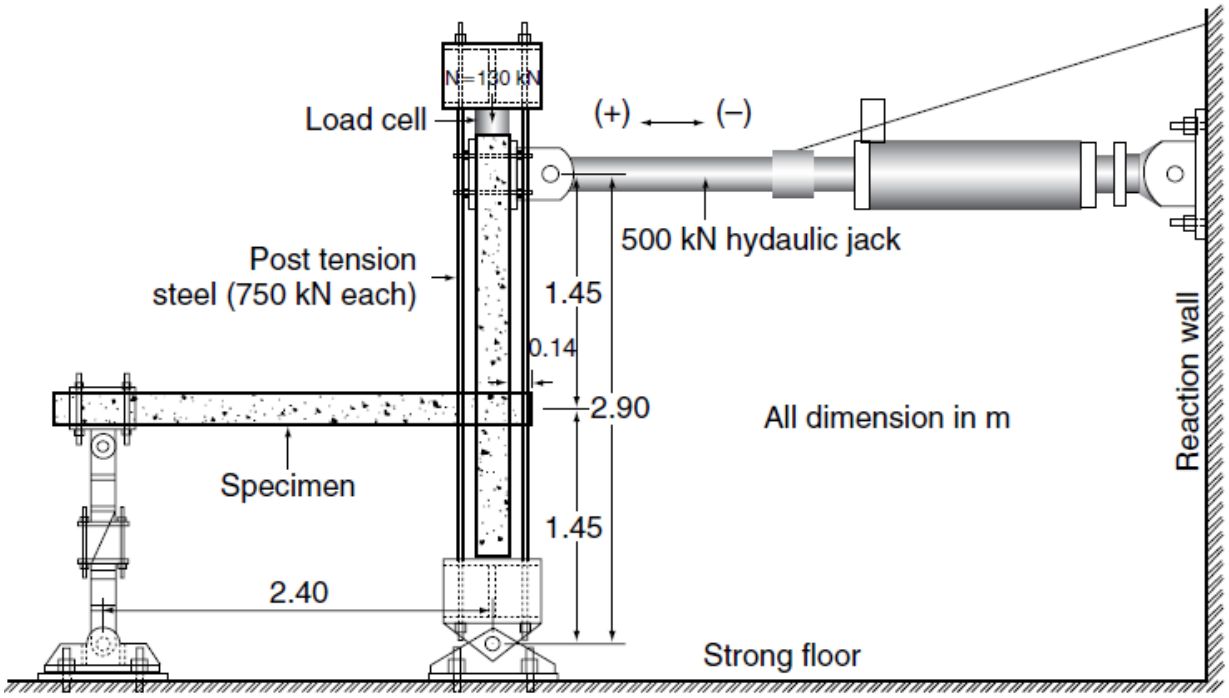
N=130 kN
Load cell
(+) ⟷ (−)
500 kN hydaulic jack
Post tension
steel (750 kN each)
1.45
0.14
2.90
All dimension in m
Reaction wall
Specimen
1.45
2.40
Strong floor

Fig. 4

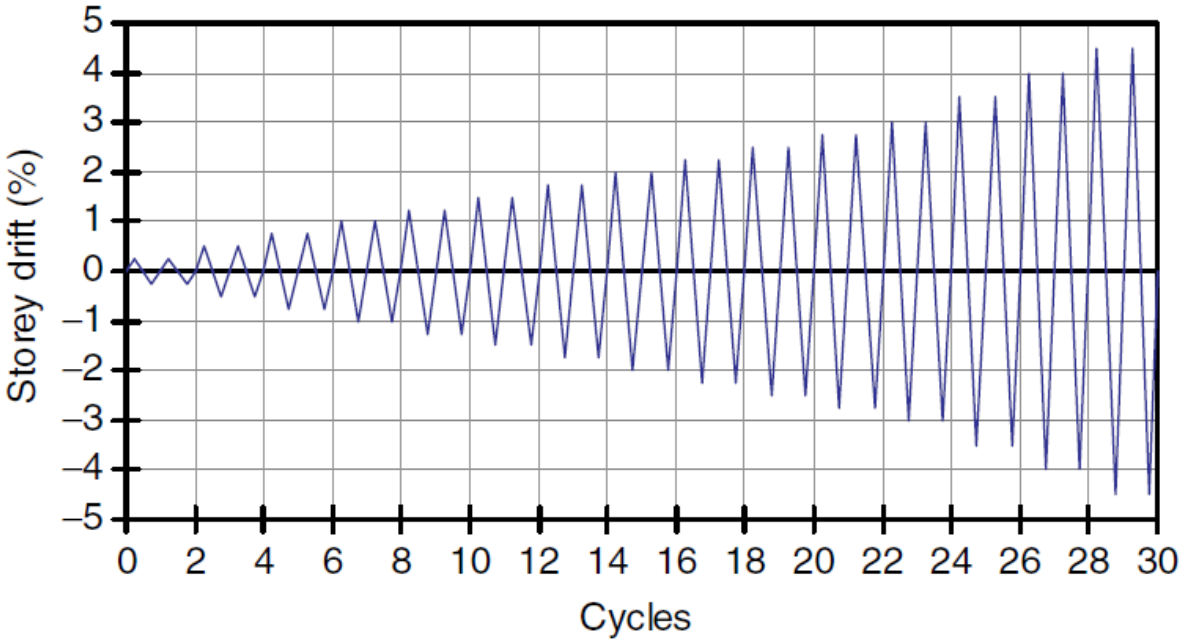
Storey drift (%)
5
4
3
2
1
0
−1
−2
−3
−4
−5
0
2
4
6
8
10
12
14
16
18
20
22
24
26
28
30
Cycles

Fig. 5

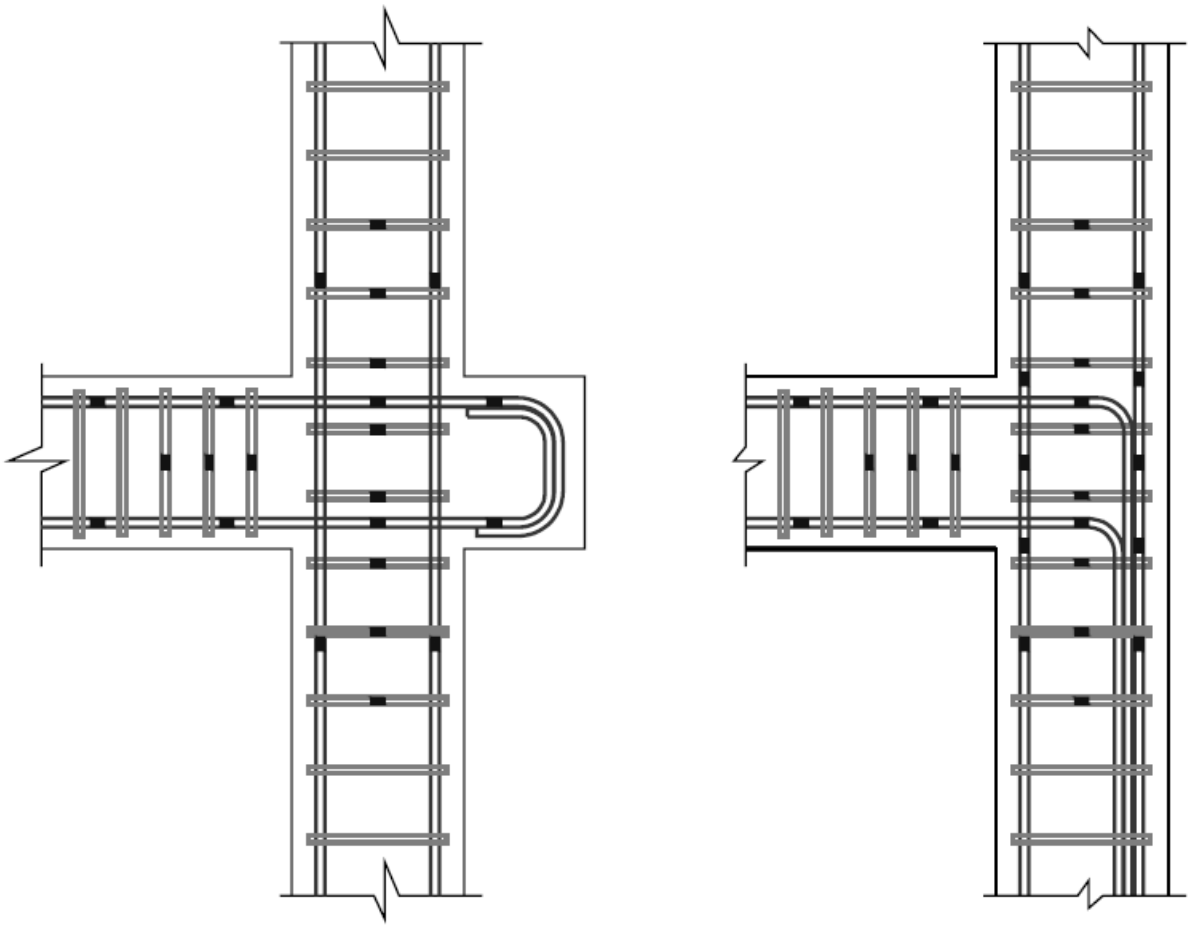

Fig. 6

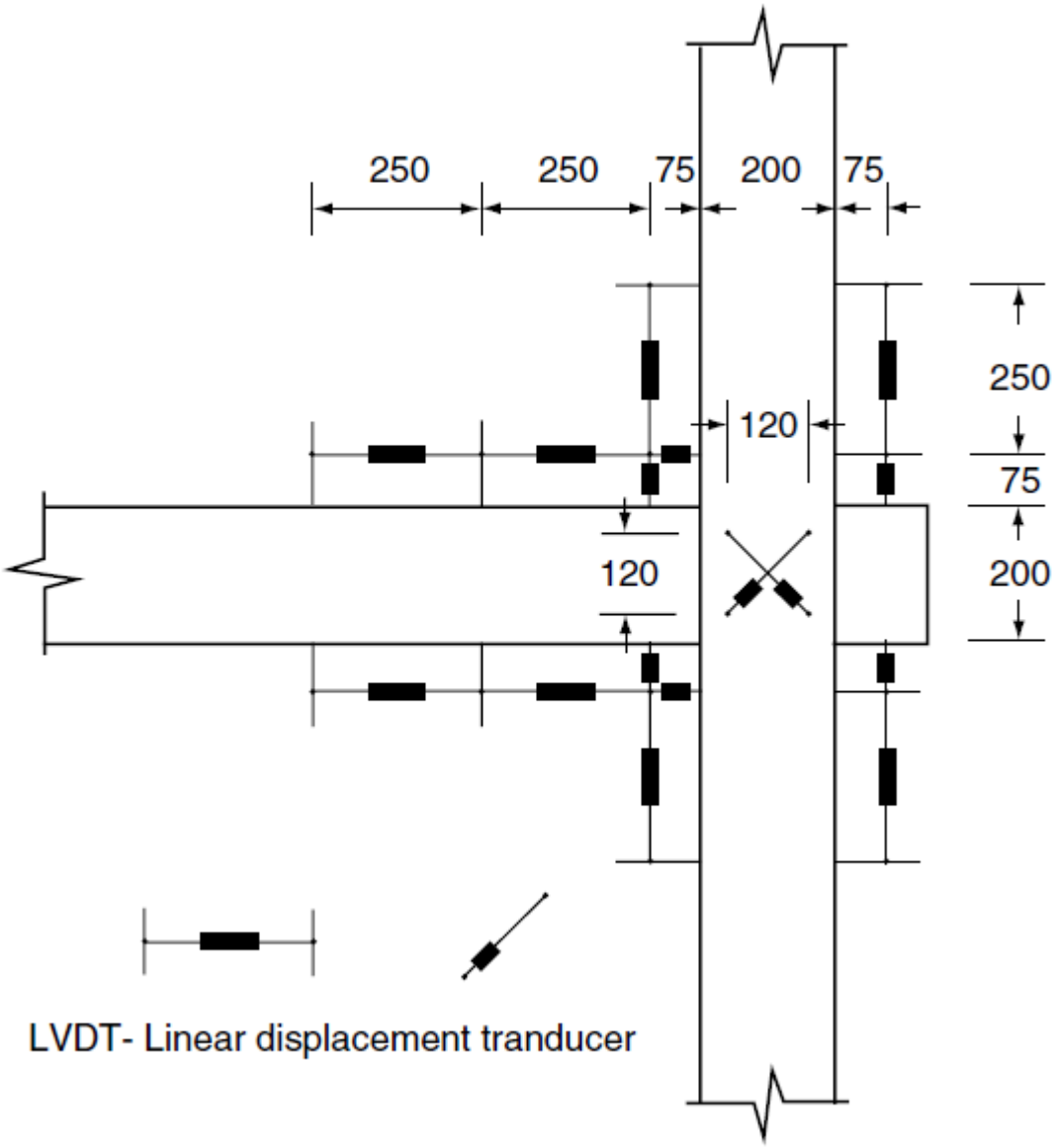
250
250
75
200
75
250
120
75
120
200
LVDT- Linear displacement tranducer

Fig. 7

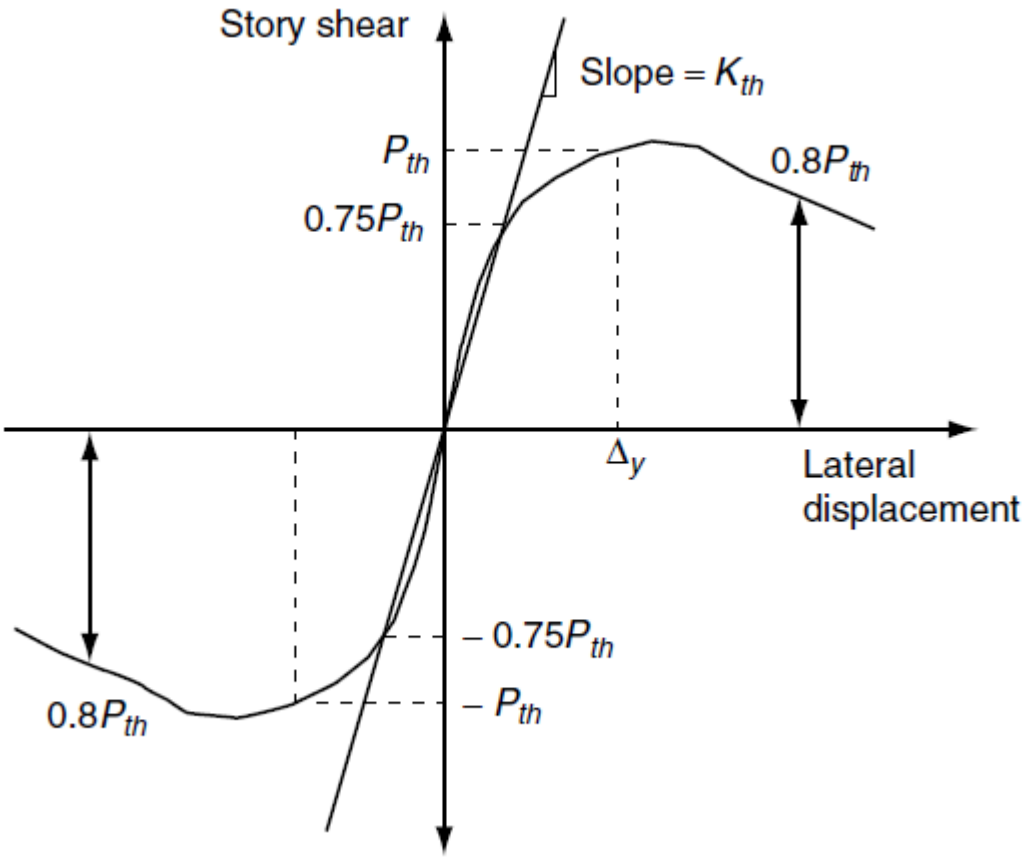
Story shear
Slope = K_{th}
P_{th}
$0.75P_{th}$
$0.8P_{th}$
Δ_y
Lateral displacement
$-0.75P_{th}$
$-P_{th}$
$0.8P_{th}$

Fig. 8

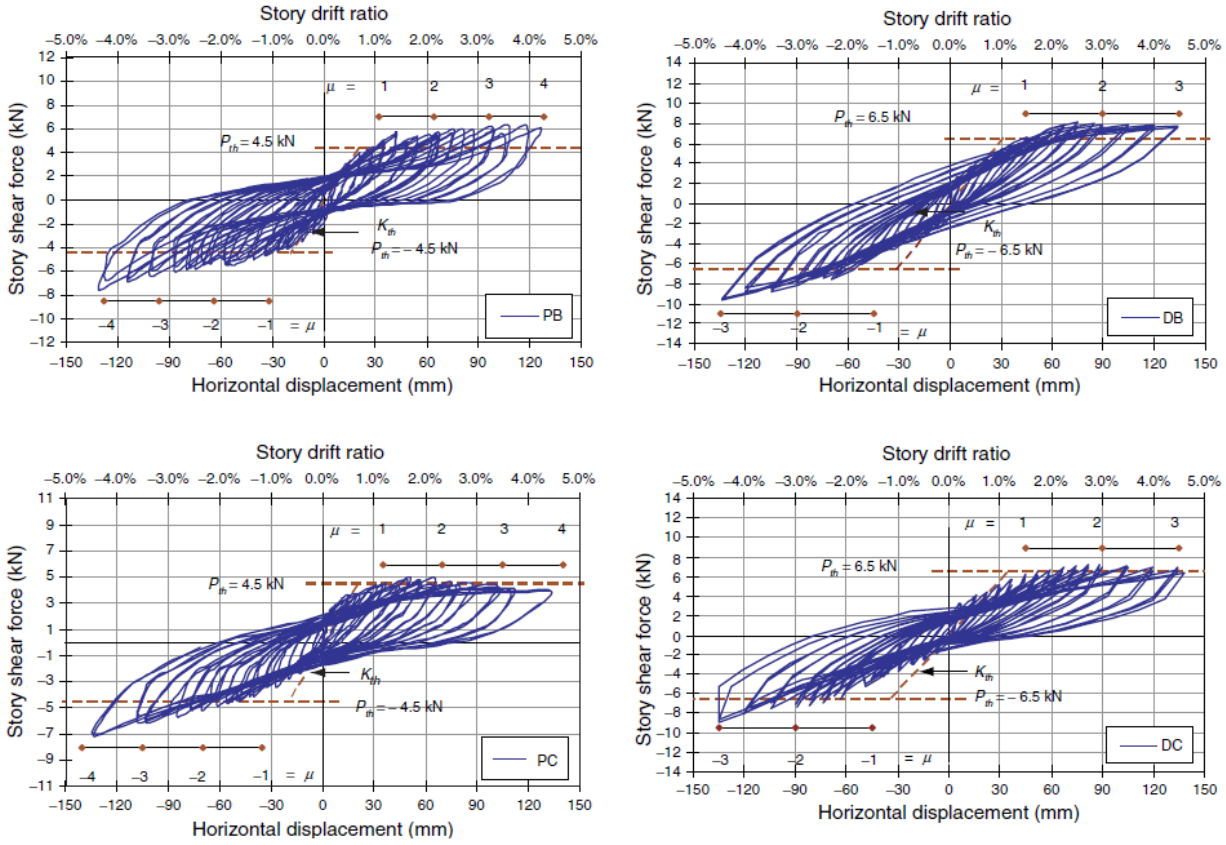
Story drift ratio
Story shear force (kN)
Horizontal displacement (mm)
P_{th} = 4.5 kN
P_{th} = −4.5 kN
K_{th}
PB
Story drift ratio
Story shear force (kN)
Horizontal displacement (mm)
P_{th} = 6.5 kN
P_{th} = −6.5 kN
K_{th}
DB
Story drift ratio
Story shear force (kN)
Horizontal displacement (mm)
P_{th} = 4.5 kN
P_{th} = −4.5 kN
K_{th}
PC
Story drift ratio
Story shear force (kN)
Horizontal displacement (mm)
P_{th} = 6.5 kN
P_{th} = −6.5 kN
K_{th}
DC

Fig. 9

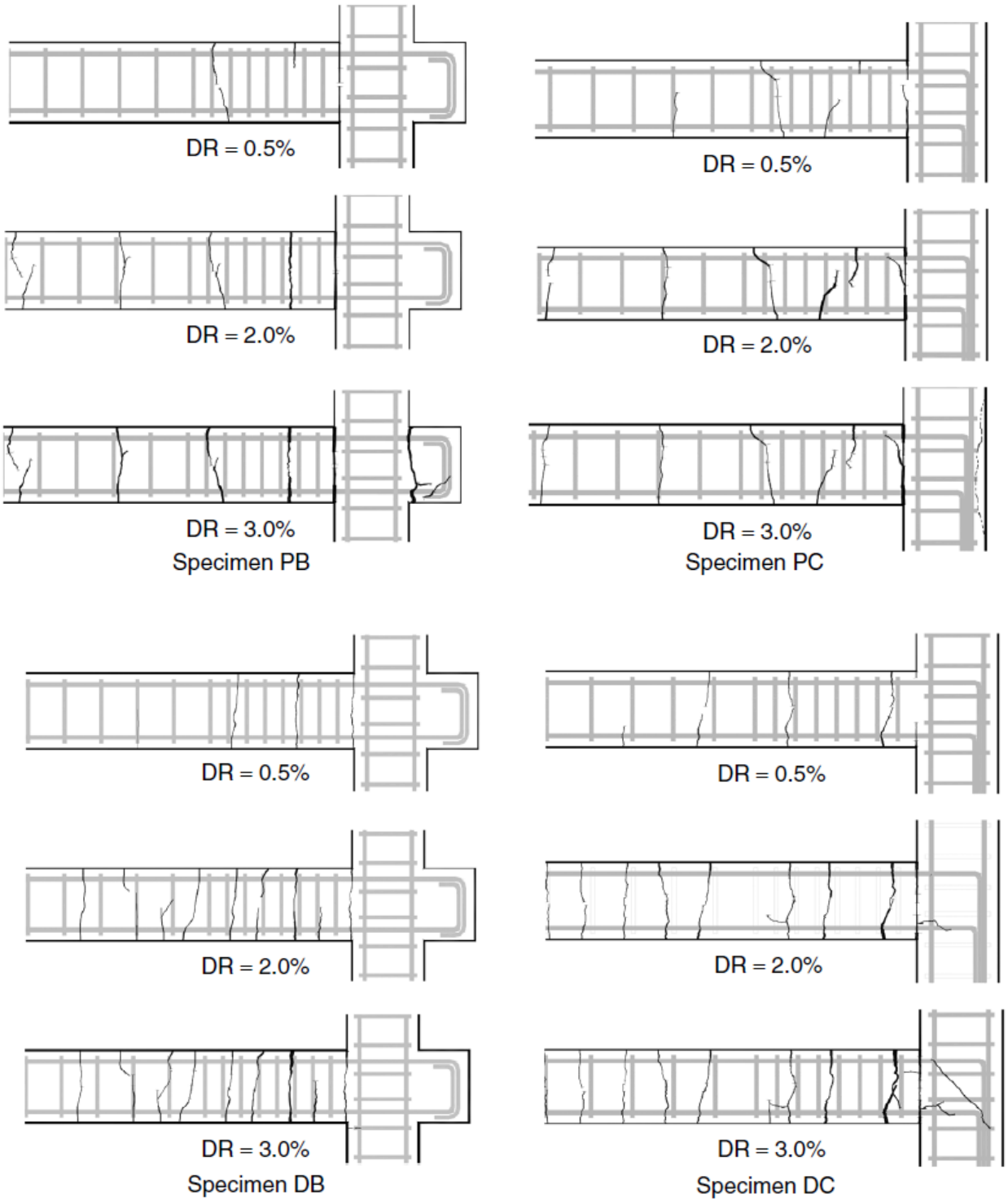
DR = 0.5%
DR = 2.0%
DR = 3.0%
Specimen PB
DR = 0.5%
DR = 2.0%
DR = 3.0%
Specimen PC
DR = 0.5%
DR = 2.0%
DR = 3.0%
Specimen DB
DR = 0.5%
DR = 2.0%
DR = 3.0%
Specimen DC

Fig. 10

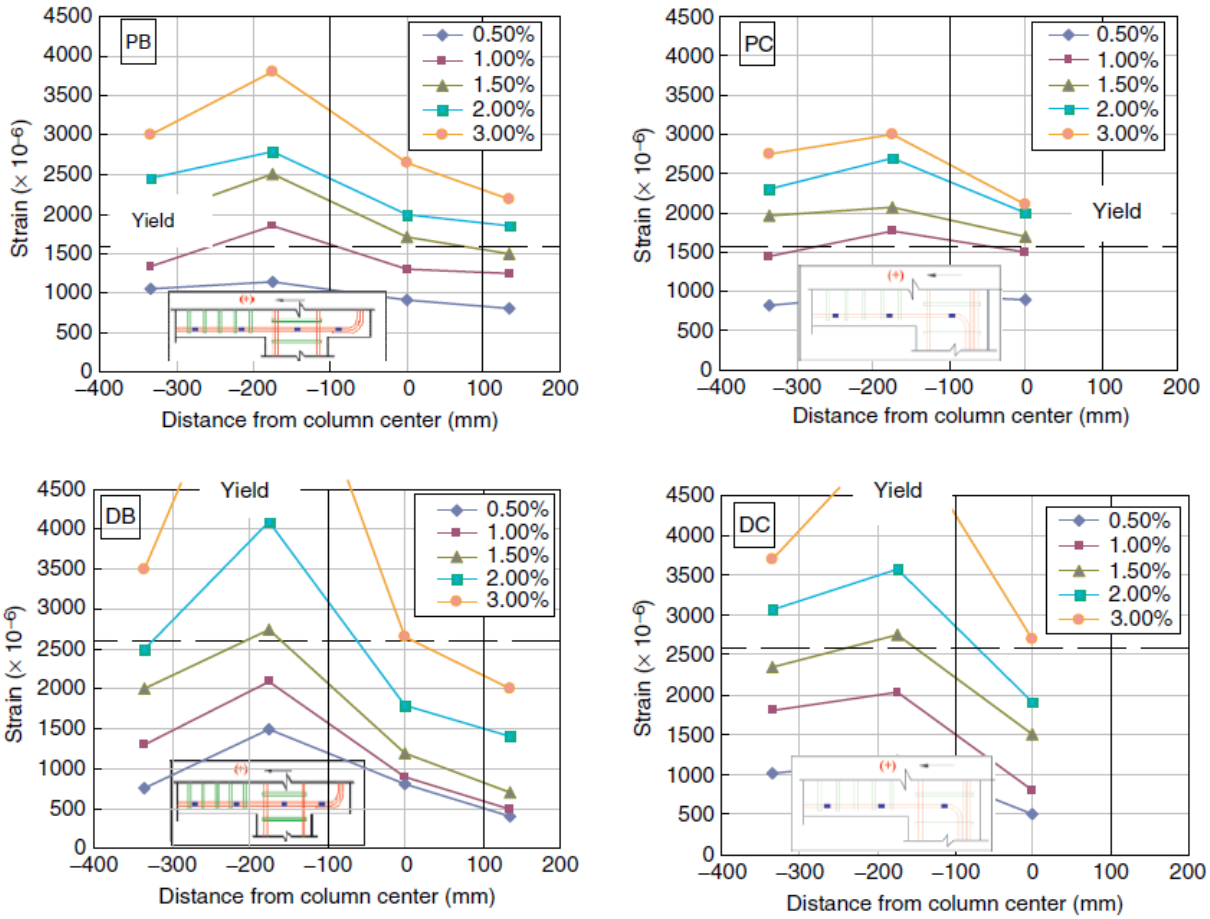
PB
PC
DB
DC
0.50%
1.00%
1.50%
2.00%
3.00%
Yield
Strain (× 10⁻⁶)
Distance from column center (mm)
4500
4000
3500
3000
2500
2000
1500
1000
500
0
–400
–300
–200
–100
0
100
200

Fig. 11

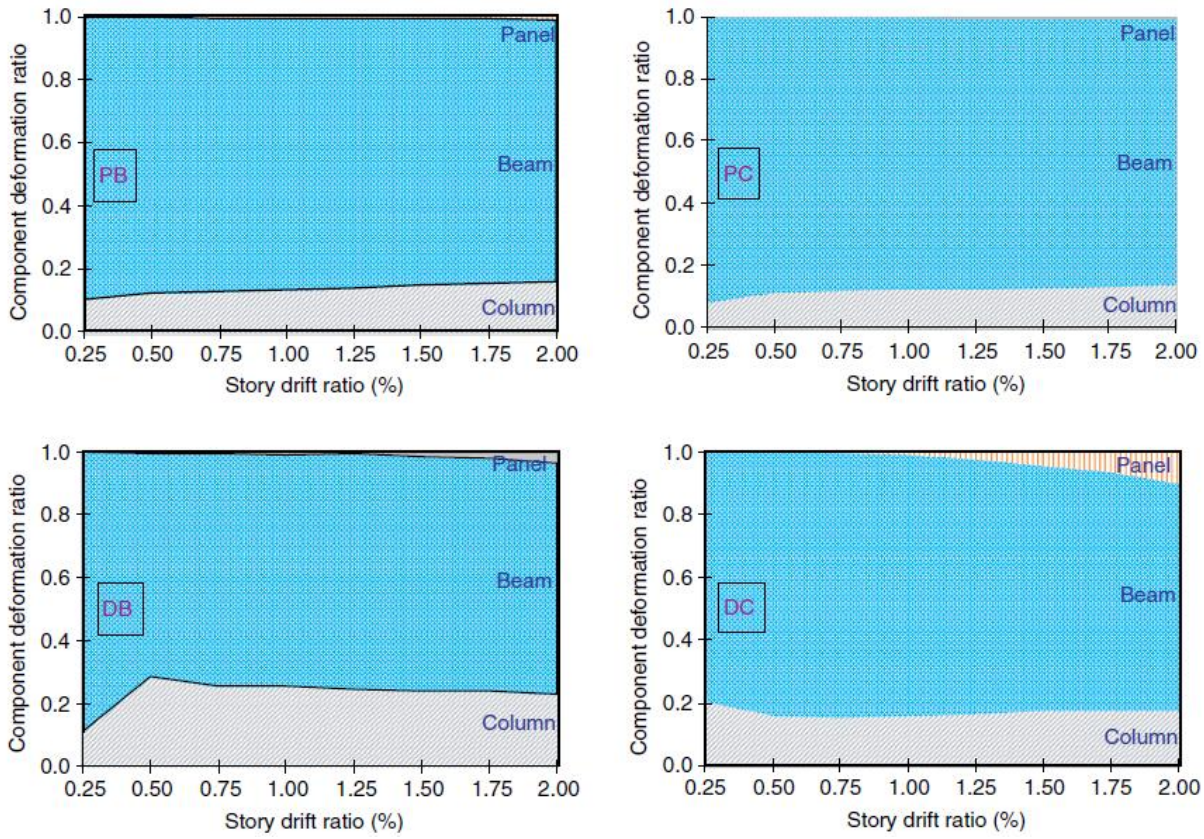
Component deformation ratio
Story drift ratio (%)
PB
PC
DB
DC
Panel
Beam
Column
0.0
0.2
0.4
0.6
0.8
1.0
0.25
0.50
0.75
1.00
1.25
1.50
1.75
2.00

Fig. 12

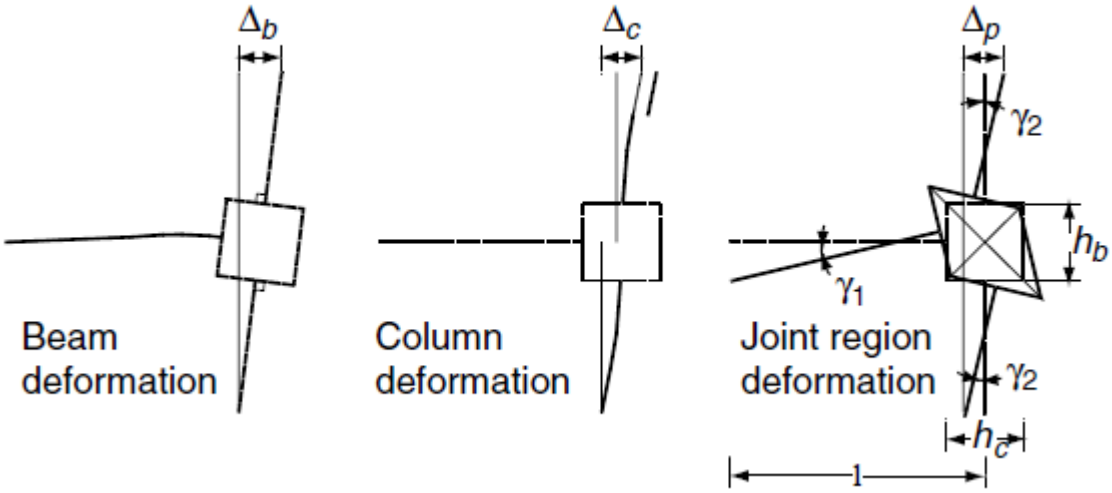
Δ_b
Δ_c
Δ_p
γ_2
h_b
γ_1
Beam deformation
Column deformation
Joint region deformation
γ_2
h_c
1

Fig. 13

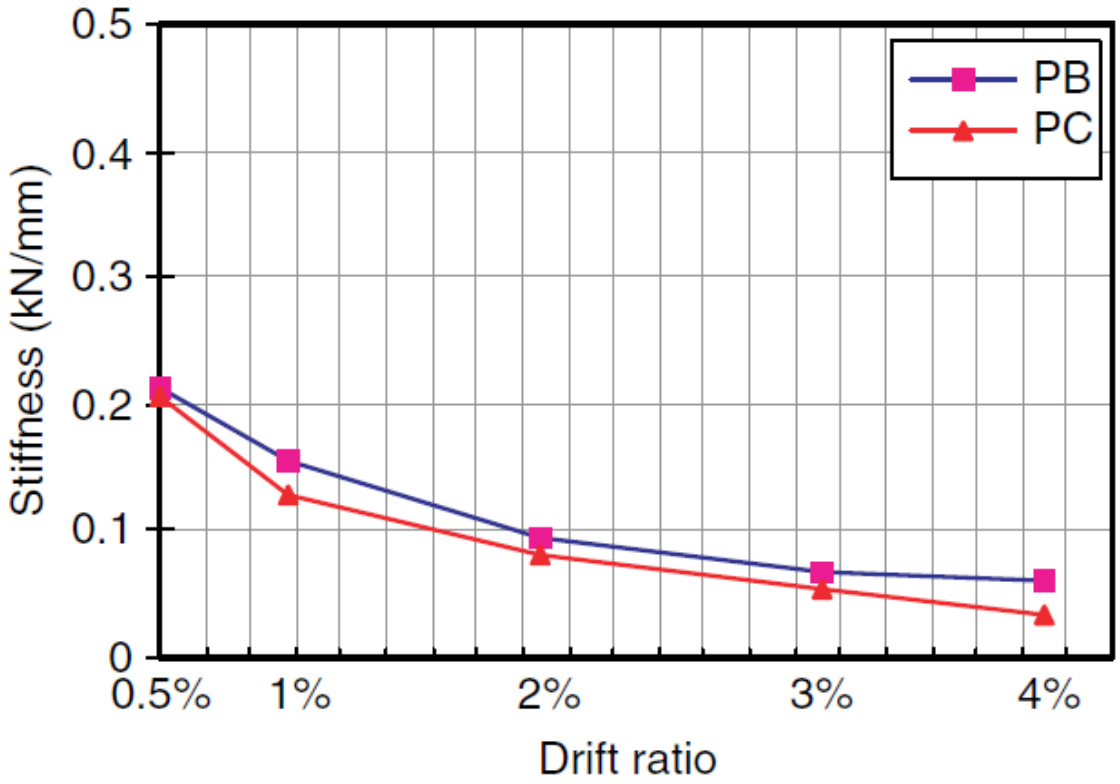

Fig. 14

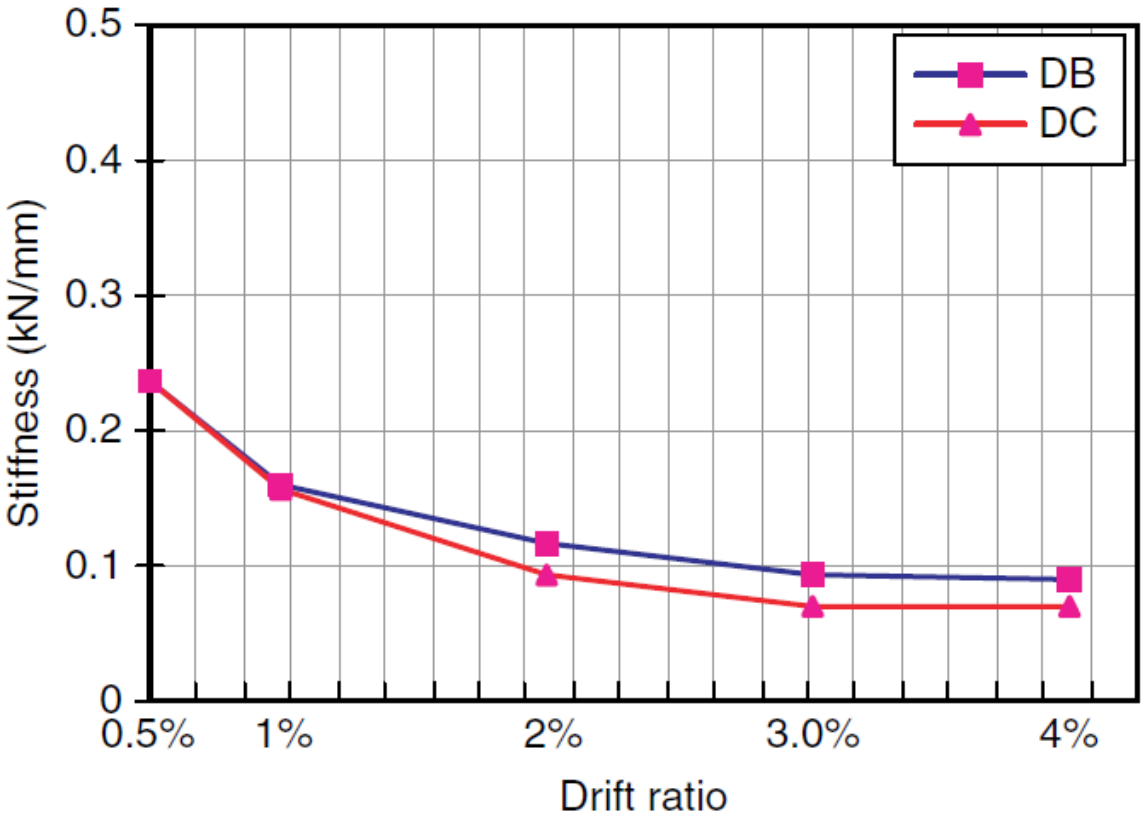

Fig. 15

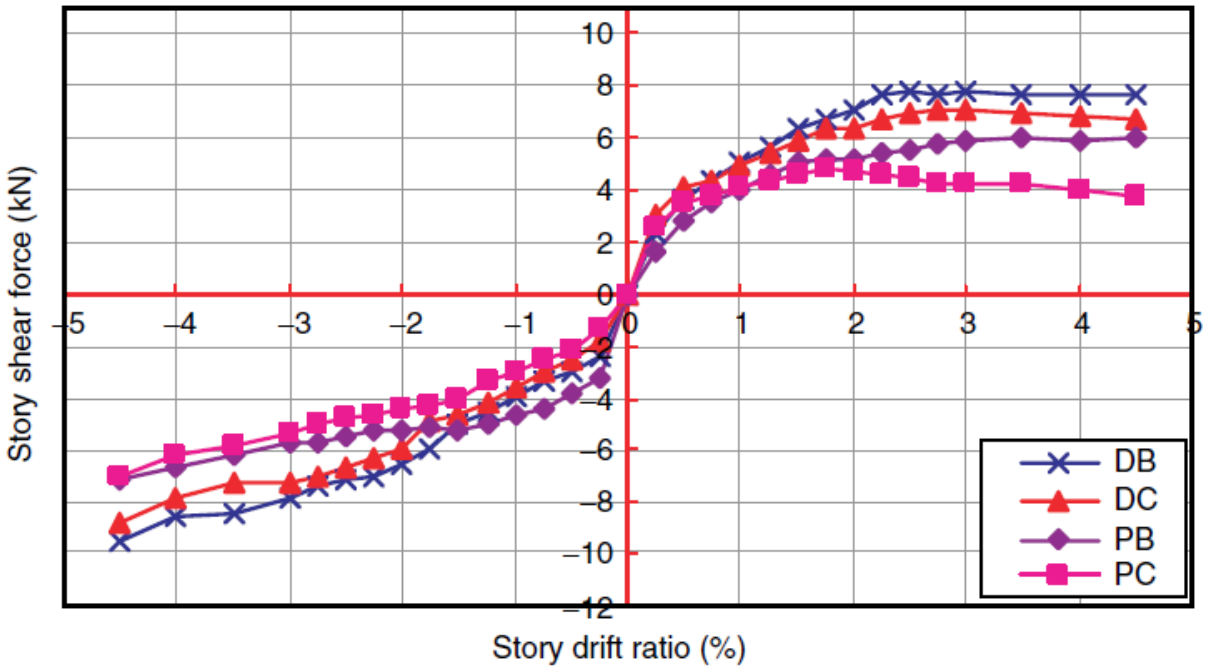
Story shear force (kN)
10
8
6
4
2
0
−2
−4
−6
−8
−10
−12
−5
−4
−3
−2
−1
0
1
2
3
4
5
Story drift ratio (%)
DB
DC
PB
PC

Fig. 16

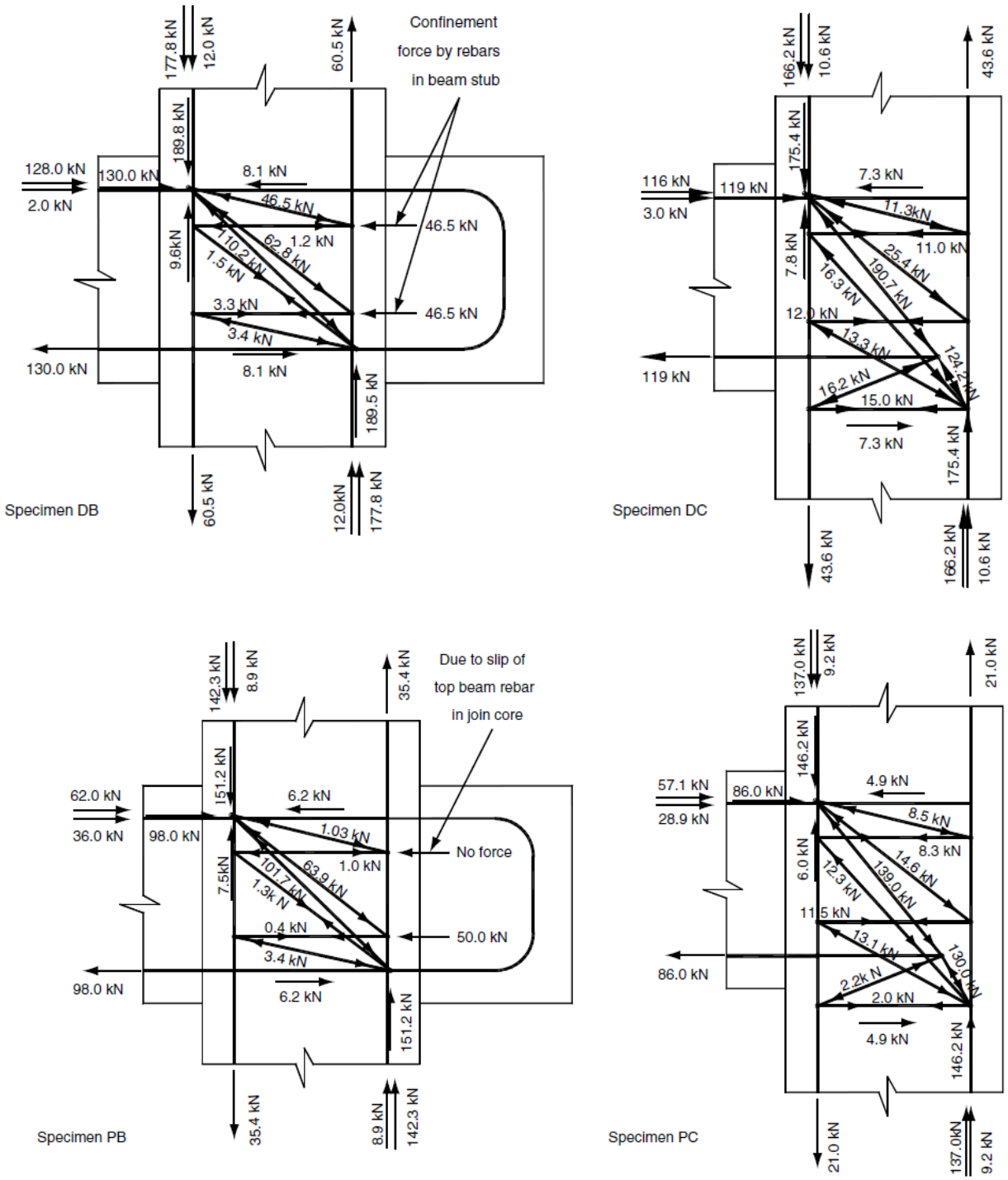
Confinement
force by rebars
in beam stub
177.8 kN
12.0 kN
60.5 kN
189.8 kN
128.0 kN
130.0 kN
2.0 kN
8.1 kN
46.5 kN
46.5 kN
9.6kN
110.2 kN
62.8 kN
1.2 kN
1.5 kN
3.3 kN
46.5 kN
3.4 kN
130.0 kN
8.1 kN
189.5 kN
60.5 kN
12.0kN
177.8 kN
Specimen DB
166.2 kN
10.6 kN
43.6 kN
175.4 kN
116 kN
119 kN
3.0 kN
7.3 kN
11.3kN
11.0 kN
7.8 kN
25.4 kN
16.3 kN
190.7 kN
12.0 kN
13.3 kN
119 kN
16.2 kN
15.0 kN
7.3 kN
175.4 kN
43.6 kN
166.2 kN
10.6 kN
Specimen DC
142.3 kN
8.9 kN
35.4 kN
Due to slip of
top beam rebar
in join core
151.2 kN
62.0 kN
36.0 kN
98.0 kN
6.2 kN
1.03 kN
No force
1.0 kN
7.5kN
101.7 kN
63.9 kN
1.3k N
0.4 kN
50.0 kN
3.4 kN
98.0 kN
6.2 kN
151.2 kN
35.4 kN
8.9 kN
142.3 kN
Specimen PB
137.0 kN
9.2 kN
21.0 kN
146.2 kN
57.1 kN
28.9 kN
86.0 kN
4.9 kN
8.5 kN
8.3 kN
6.0 kN
14.6 kN
12.3 kN
139.0 kN
11.5 kN
13.1 kN
86.0 kN
2.2k N
2.0 kN
4.9 kN
146.2 kN
21.0 kN
137.0kN
9.2 kN
Specimen PC

Fig. 17

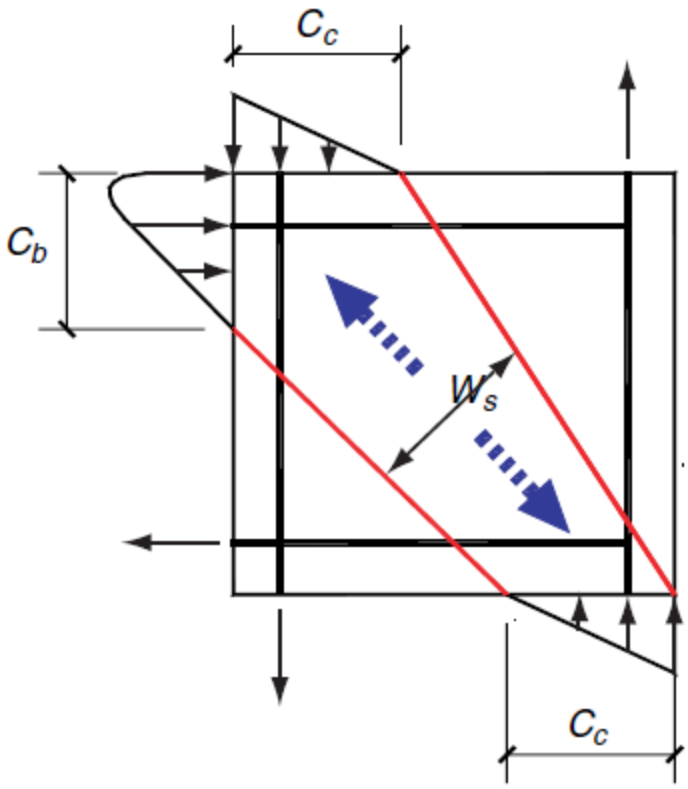

Fig. 18